Earth and Planetary Science Letters 584 (2022) 117481

Contents lists available at ScienceDirect

Earth and Planetary Science Letters

www.elsevier.com/locate/epsl

Fill, flush or shuffle: How is sediment carried through submarine channels to build lobes?

Maarten S. Heijnen [a,b], Michael A. Clare [a,*], Matthieu J.B. Cartigny [c], Peter J. Talling [c], Sophie Hage [d], Ed L. Pope [c], Lewis Bailey [b], Esther Sumner [b], D. Gwyn Lintern [e], Cooper Stacey [e], Daniel R. Parsons [f], Stephen M. Simmons [f], Ye Chen [f], Stephen M. Hubbard [d], Joris T. Eggenhuisen [g], Ian Kane [h], John E. Hughes Clarke [i]

[a] National Oceanography Centre Southampton, European Way, Southampton, SO14 3ZH, UK
[b] School of Ocean and Earth Sciences, University of Southampton, European Way, Southampton, SO14 3ZH, UK
[c] Departments of Earth Science and Geography, Durham University, Science Laboratories, South Road, Durham, DH1 3LE, UK
[d] Univ Brest, CNRS, Ifremer, Geo-Ocean, F-29280 Plouzané, France
[e] Natural Resources Canada, Geological Survey of Canada, 9860 W Saanich Road, V8L 4B2, Sidney, BC, Canada
[f] Energy and Environment Institute, University of Hull, HU6 7RX, UK
[g] Faculty of Geosciences, Utrecht University, Princetonlaan 8a, 3584 CB Utrecht, the Netherlands
[h] School of Earth and Environmental Sciences, University of Manchester, Manchester M13 9PL, UK
[i] Center for Coastal and Ocean Mapping, University of New Hampshire, 24 Colovos Road, Durham, NH 03824, USA

ARTICLE INFO

Article history:
Received 1 October 2021
Received in revised form 9 February 2022
Accepted 1 March 2022
Available online xxxx
Editor: J.-P. Avouac

Keywords:
submarine channel
turbidity current
flushing
source to sink
bypass
lobe

ABSTRACT

Submarine channels are the primary conduits for land-derived material, including organic carbon, pollutants, and nutrients, into the deep-sea. The flows (turbidity currents) that traverse these systems can pose hazards to seafloor infrastructure such as cables and pipelines. Here we use a novel combination of repeat seafloor surveys and turbidity current monitoring along a 50 km-long submarine channel in Bute Inlet, British Columbia, and discharge measurements from the main feeding river. These source-to-sink observations provide the most detailed information yet on magnitude-frequency-distance relationships for turbidity currents, and the spatial-temporal patterns of sediment transport within a submarine channel-lobe system. This analysis provides new insights into mass redistribution, and particle residence times in submarine channels, as well as where particles are eventually buried and how that is recorded in the deposits. We observe stepwise sediment transport down the channel, with turbidity currents becoming progressively less frequent with distance. Most flows dissipate and deposit within the proximal (< 11 km) part of the system, whilst longer run-out flows then pick up this sediment, 'shuffling' it further downstream along the channel. This shuffling occurs mainly through upstream migration of knickpoints, which can generate sediment bypass along the channel over timescales of 10–100 yrs. Infrequent large events flush the channel and ultimately transport sediment onto the lobe. These flushing events can occur without obvious triggers, and thus might be internally generated. We then present the first ever sediment budget analysis of an entire submarine channel system, which shows that the river input and lobe aggradation can approximately balance over decadal timescales. We conclude by discussing the implication of this sediment shuffling for seafloor geohazards and particle burial.

1. Introduction

Submarine channels are the primary conduits for terrestrial and coastal-derived material to the deep-sea, forming the world's largest sediment accumulations (Curray et al., 2002). Some of the most important questions about sediment transport through submarine channels concern the spatial and temporal patterns of sediment transport, the magnitude-frequency distribution of flows responsible for these patterns, how these patterns and this distribution vary along-system and over time, and how they are manifested in the stratigraphic record. These are also fundamental questions for other types of sediment transport system (e.g. rivers, alluvial fans, and landslide systems). This relationship between event magnitude-frequency, and its variation with distance, governs how

* Corresponding author.
E-mail address: michael.clare@noc.ac.uk (M.A. Clare).

https://doi.org/10.1016/j.epsl.2022.117481

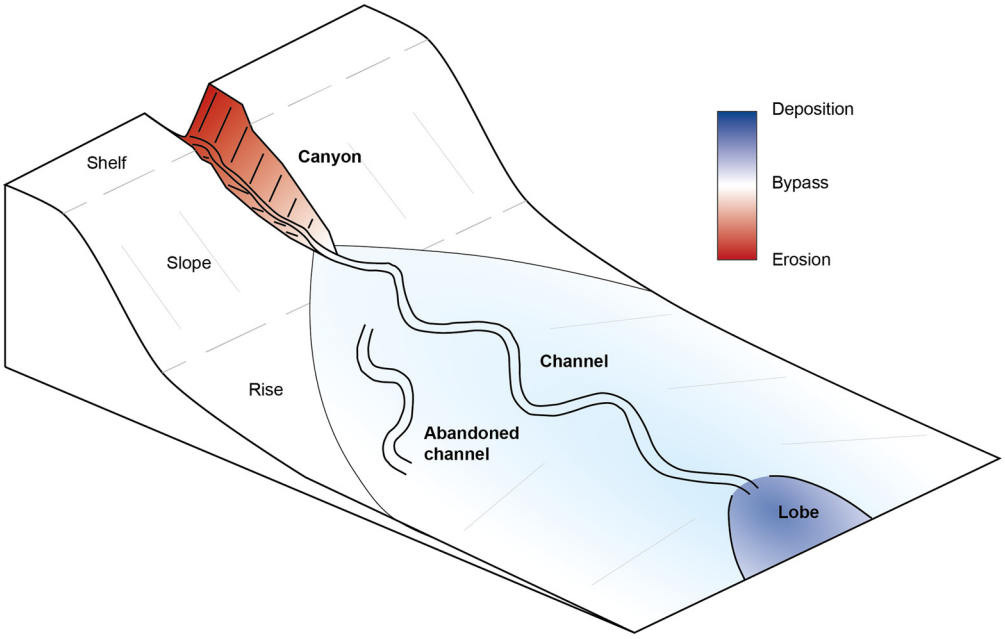

Fig. 1. Generalised models of how submarine channel systems evolve over longer timescales showing how erosion and deposition is distributed over longer timescales in a submarine channel system. The upstream canyon is characterised by erosion, the channel by bypass or slight deposition and the lobe is depositional (redrawn from Wells and Cossu, 2013). (For interpretation of the colours in the figure(s), the reader is referred to the web version of this article.)

mass is redistributed. For submarine settings, this relationship determines the hazards faced by the global network of seafloor cables (Carter et al., 2009; Heezen and Ewing, 1952). It also determines residence times of sediment grains at a site, and whether they will become exhumed; thus influencing the supply of nutrients, and pollutants to marine food webs, and efficiency of organic carbon burial in marine sediments (Azaroff et al., 2020; Baudin et al., 2010; Canals et al., 2006; De Leo et al., 2010; Pierdomenico et al., 2020). Finally, the magnitude-frequency relationship and resulting depositional/erosional patterns determine how deposits are formed, and what is ultimately recorded. This is important as submarine channel and lobe deposits are used as archives of Earth history, including past climates or geohazards such as earthquakes, floods, and storms (Prins and Postma, 2000; St.-Onge et al., 2004; Masson et al., 2011).

Direct observation of sediment transport through submarine channel systems has been challenging, because of the often-remote locations, and the destructive and episodic nature of turbidity currents (Hughes Clarke, 2016; Inman et al., 1976; Paull et al., 2018). Studies of sediment volume budgets, or changes in flow magnitude-frequency are sparse, and fewer still integrate monitoring of flows and seafloor change (Stacey et al., 2019). We therefore rely upon inferences from deposits left behind by turbidity currents, scaled-down laboratory models, numerical models, or individual seafloor surveys (de Leeuw et al., 2016; Hubbard et al., 2020; Paull et al., 2011; Sylvester et al., 2011). These studies underpin a classical view of submarine canyon-channel-lobe systems over long (100s->100,000s of years) timescales (Fig. 1), wherein the upstream and deeply incised part of systems ('canyons') are characterised by long-term erosion (Fig. 1; Shepard, 1981; Carlson and Karl, 1988). Submarine channels that extend from canyons are typically characterised by areas of less severe erosion, sediment bypass (where erosion balances deposition), or gradual aggradation (Normark, 1970; Stevenson et al., 2015). Some submarine channel systems are fed directly at a river-mouth, where a prodelta, rather than a well-developed canyon, transitions downslope into a channel (e.g. Heijnen et al., 2020). Lobes are the downstream termini of submarine channels, which are dominantly depositional areas (Jobe et al., 2018; Normark, 1970).

Competing models exist for how flow frequency and magnitude change with distance along submarine channel-lobe systems, and the resultant long-term spatial variations in erosion or deposition (Fig. 2). The first model assumes individual flows transition from net-erosive in the canyon, to mainly bypassing in the channel, and depositional on the lobe (Fig. 2a). In this 'ignition-autosuspension-deposition' model, an initial catastrophic event (earthquake, flood, storm) generates a powerful turbidity current in the canyon (Heezen and Ewing, 1952; Jobe et al., 2018; Masson et al., 2011; Mountjoy et al., 2018; Normark and Piper, 1991; Sequeiros et al., 2019; St.-Onge et al., 2004). These turbidity currents erode and entrain sediment proximally, increasing their density and ability to erode; a positive feedback called ignition (Bagnold, 1962; Parker et al., 1986). Flows may reach an equilibrium state, where seabed erosion and deposition approximately balance, termed 'autosuspension' (Bagnold, 1962; Heerema et al., 2020; Parker et al., 1986; Stevenson et al., 2015). Autosuspending flows carry their sediment load through the channel without significant erosion or deposition (also called 'bypassing' flow), before depositing the transported sediment primarily on the lobe, where flow is less confined (Fig. 2a). The long-term pattern of seabed erosion, bypass, and deposition is thus mirrored by comparable changes with distance within each individual flow (Fig. 2a). This simplistic model implicitly assumes the system is repeatedly traversed by a single magnitude of flows, which have broadly comparable behaviour, and all are recorded in the lobe deposits.

A second 'fill-and-flush' model assumes more frequent, weaker and shorter runout flows fill the proximal part of a submarine canyon or channel; whilst more powerful and longer runout flows occasionally flush sediment through the whole system to the lobe (Fig. 2b; Normark and Piper, 1991; Allin et al., 2016). As in the 'ignition-autosuspension-deposition' model, flushing flows have been linked to catastrophic triggering events (e.g. major earthquakes, floods, or typhoons; St.-Onge et al., 2004; Masson et al., 2011; Mountjoy et al., 2018; Sequeiros et al., 2019). This second model differs from the first, as long-term patterns of seabed erosion and deposition are not mirrored by erosion-deposition patterns in all flows; however, flushing flows in this model could

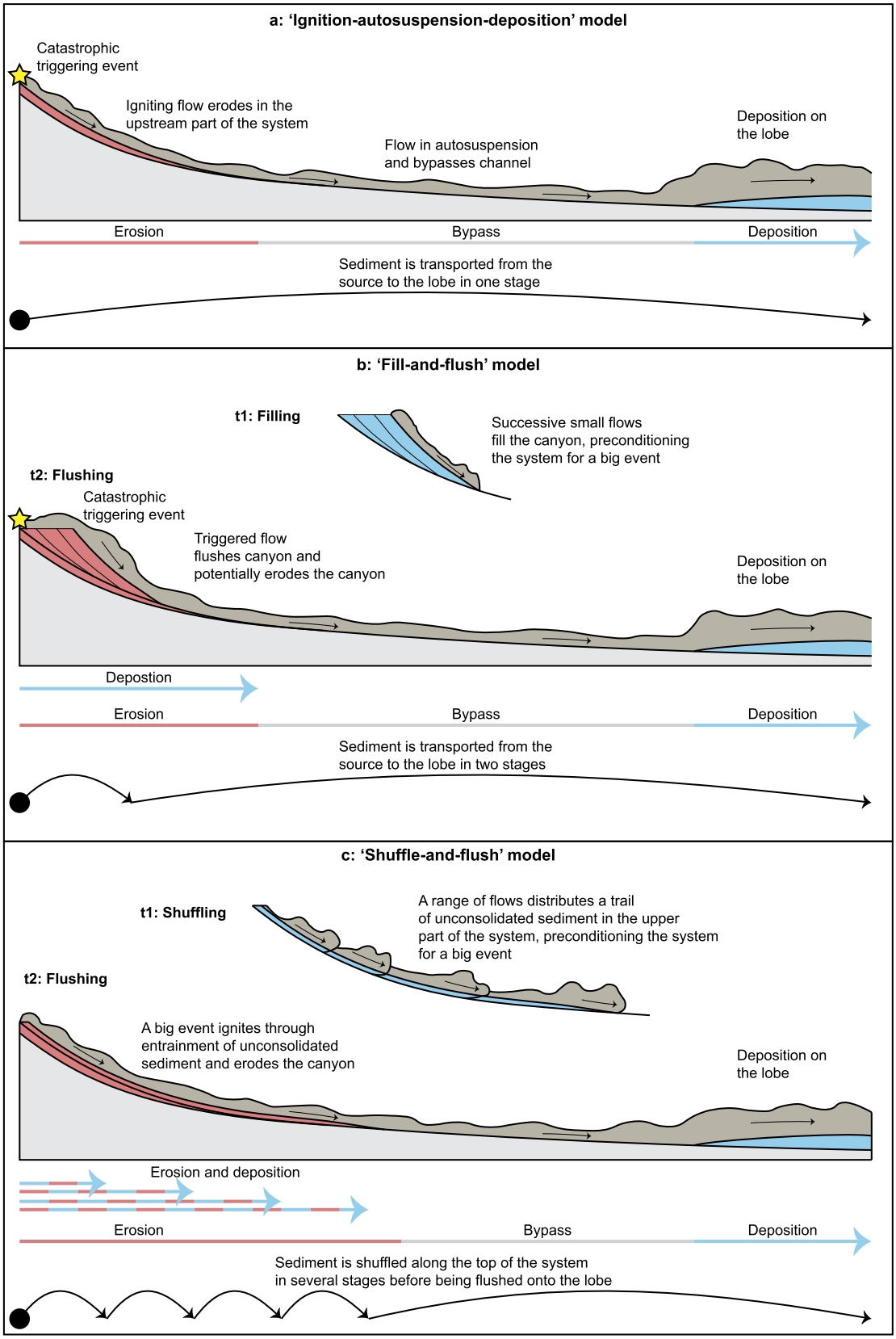

Fig. 2. Three different models of sediment transport through submarine channel systems. a) Autosuspension model: a single big flow triggered by a catastrophic event erodes in the canyon, then reaches a state of autosuspension and bypasses the channel, and deposits its sediment on the lobe. b) Fill-and-flush model: frequent successive small flows fill the upper canyon, preconditioning a large flow triggered by a catastrophic event. This large flow then flushes this preconditioned sediment and ignites, then bypasses the channel and deposits on the lobe. c) Shuffle-and-flush model: successive flows decreasing in frequency with distance, distribute a trail of unconsolidated sediment in the upper part of the system. A larger turbidity current is generated as it picks up this sediment, balancing out the original deposition in the channel before depositing on the lobe.

broadly resemble flows in the 'ignition-autosuspension-deposition' model (Fig. 2a).

The third 'shuffle-and-flush' model is a modified version of the 'fill-and-flush' model, where instead sediment travels through the canyon-channel in multiple steps (Paull et al., 2005). Sediment is repeatedly buried, excavated and transported progressively down-channel by flows of variable run-out length, which varies as a function of flow frequency (Paull et al., 2005; Stacey et al., 2019). These 'shuffling' flows may lead to complex patterns of alternating deposition and erosion over shorter timescales. It remains unclear whether flushing flows come from the same overall magnitude-frequency distribution as shuffling flows, representing the tail of that distribution; or if they are a separate class with distinct triggers. In both 'fill-and-flush' and 'shuffle-and-flush' models, lobe deposits hold an incomplete record of the activity of the system, as only the flushing flows are recorded. A lack of source-to-sink monitoring studies means that these models remain untested at field-scale. Here we present the first direct monitoring dataset for an active submarine channel-lobe system along its full length to test these three models of submarine channel and lobe activity.

2. Aims

Our overarching aim is to understand the spatial and temporal patterns of sediment transport, and magnitude-frequency-distance relationships of turbidity currents, within a submarine channel system. We address the following specific aims using data collected from a 50 km-long channel and associated lobe in Bute Inlet, Canada. The first aim is to understand how patterns of erosion and deposition vary spatially along the channel, and over different timescales. The second is to determine when and how efficiently sediment is delivered to the terminal lobe and what controls the timing of this sediment delivery. Previous studies suggested catastrophic triggers such as floods and/or earthquakes are required, but here we explore whether sediment delivery to the lobe can occur without major external triggers. The third is to provide the first detailed budget analysis of sediment sources and sinks within an entire submarine channel-lobe system. The fourth is to use these results to test three general and fundamental models (Fig. 2) for sediment transport through submarine channels, including the relationship between magnitude-frequency-distance of submarine flows, and how sediment bypasses submarine channels. Finally, we discuss wider implications for organic carbon, nutrient and pollutant transfer to the deep-sea, whether lobes record floods or other hazards, and how lobe deposits are built in the stratigraphic record.

3. Field monitoring site

We analyse data from the 50 km-long submarine channel system in Bute Inlet, British Columbia, Canada (Fig. 3a, b; Prior et al., 1987; Zeng et al., 1991). The submarine channel system extends from the prodeltas of the Homathko and Southgate Rivers, to a lobe at 650 m water depth (Fig. 3b). The Homathko River is responsible for 70–80% of the freshwater input, the Southgate River provides 15–25%, while small streams on the sides of the fjord account for the remaining 5% (Syvitski and Farrow, 1983; Zeng et al., 1991). The submarine channel has an average gradient of 0.6° and sinuosity of 1.4. The uppermost channel reaches slopes of up to 3°, while the gradient at the lobe is ~0.1° (Chen et al., 2021; Heijnen et al., 2020; Zeng et al., 1991). The channel floor mainly comprises sand, while overbank areas are dominantly silty at seafloor (Zeng et al., 1991). Sandy turbidites occur in the subsurface in overbank areas (Chen et al., 2021; Zeng et al., 1991). Tens of turbidity currents occur each year in the upper reach of the channel, during the summer freshet, when the Homathko River discharge rises above 200 m^3/s due to snowmelt (Chen et al., 2021; Prior et al., 1987; Zeng et al., 1991). The submarine channel is mostly inactive during the winter, when river discharges are below 100 m^3/s (Prior et al., 1987). Repeated seafloor surveys a few years apart have shown how turbidity currents shape the seafloor, creating crescentic bedforms, and locally driving the upstream-migration of 10-40 m-high knickpoints (Chen et al., 2021; Heijnen et al., 2020).

4. Methods

Our monitoring approach integrates a decade of repeat seafloor surveys across the entire Bute Inlet channel-lobe system, direct monitoring of turbidity currents along the length of the system, and discharge measurements of the Homathko River.

4.1. Repeat seafloor surveying

The submarine channel system was surveyed ten times between March 2008 and November 2018 to determine seafloor changes (see supplementary Table 1 for precise timings of surveys). Multibeam echosounders were operated using Kongsberg Maritime SIS Software. Heave, roll, and pitch corrections were incorporated in the acquisition process using motion sensors, tidal corrections were performed using predicted tides, and data were processed in CARIS HIPS and SIPS software. Surveys were gridded with horizontal resolutions of 1–5 m. Vertical accuracy of the surveys is around 0.5% of the water depth (Heijnen et al., 2020). Seafloor elevation changes were quantified by creating elevation difference maps in ArcGIS (Fig. 3).

4.2. Turbidity current monitoring

Turbidity currents were monitored using Acoustic Doppler Current Profilers (ADCPs) during the summers of 2016 and 2018 (supplementary Table 1). Instruments were moored in the channel at six locations (M1–M6) between 3–42 km along-channel from the Homathko River mouth (Chen et al., 2021; Fig. 3c). Mooring locations were identical in 2016 and 2018, apart from the most upstream mooring (M6), which was positioned a further ~2 km upstream in 2018. Moorings recorded from June 9th until September 23rd in 2016, and May 14th to November 8th in 2018. Each mooring included at least one down-looking Teledyne Workhorse ADCP (300-1200 kHz), suspended above the channel to record flows passing beneath. Turbidity currents were identified by a sudden increase in velocity and backscatter (Paull et al., 2018). The ADCP on M5 failed during deployment in 2018; hence no data exist for analysis. Turbidity currents generally reached velocities between 0.7 and 4 m/s, with a maximum velocity of 6.2 m/s (Supplementary material). Individual flow durations were typically less than four hours, with thicknesses of less than 20 m.

4.3. River discharge monitoring

Discharge near the mouth of the Homathko River was monitored daily throughout the entire survey period (https://wateroffice.ec.gc.ca; station 08GD004). No river monitoring was available for the Southgate River.

4.4. Sediment budget analysis

Erosional and depositional volumes within the channel-system were derived through elevation differences from repeat seafloor surveys. Only erosion within the channel and on the lobe are considered, as the overbanks did not show erosion or deposition greater than the background noise. Uncertainty in the volumes derived from the difference maps is based on a vertical accuracy of

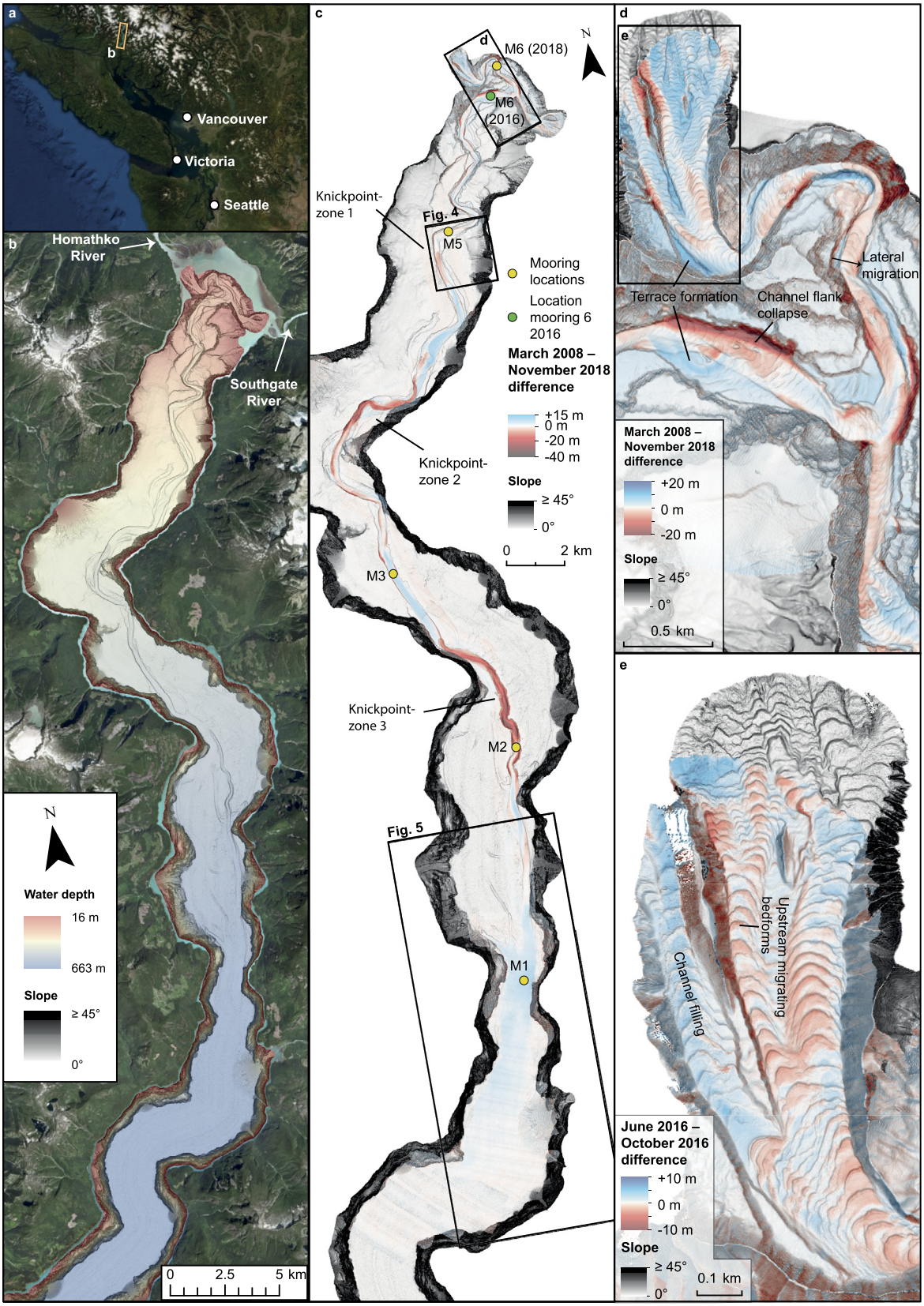

Fig. 3. Location, morphology, and change of the Bute Inlet submarine channel-lobe system. Source satellite data: Esri, DigitalGlobe, GeoEye, Earthstar, Geographics, CNES/Airbus DS, USDA, USGS, AeroGRID, IGN, and the GIS User Community. a) Location of Bute Inlet. b) Overview of the submarine channel-lobe system in Bute Inlet as monitored in March 2008. Data is presented as a slope map overlain by a semi-transparent bathymetry map. c) 2008 slope map overlain by a March 2008 – November 2018 difference map. Location of moored instrument stations is shown. Note the along-channel alternation of erosional and depositional areas controlled by knickpoints. d) Detailed difference map of the upper channel. Location shown in panel c. Note patterns of erosion and deposition caused by a variety of different processes. e) Detailed difference map over June–October 2016 of the Homathko River Prodelta. Location shown in panel d. Note the upstream-migrating bedforms dominating the evolution of the prodelta on the short timescale.

Table 1
Sediment budgets in Bute Inlet between March 2008 and November 2018. Sediment sources are sediment exhumed through erosion and sediment delivered by the Homathko River. Sediment volume delivered by the Homathko River is represented as the volume if it were deposited.

System component	Sediment sources (eroded from seabed or supplied from river mouth)	Sediment deposited on seabed
Homathko River (2008-18) (annual range of sediment supply to Bute Inlet from Syvitski and Farrow, 1983)	25–43 million m^3 (i.e. sediment supplied by the Homathko River)	-
Submarine Prodeltas & Submarine Channel (2008-18) (volume eroded or deposited during the time-lapse surveys)	41 ± 12 million m^3 (i.e. eroded volume)	19 ± 11 million m^3 (i.e. deposited volume)
March 2008 – November 2010	*13.0 ± 14 million m^3*	*7 ± 9 million m^3*
November 2010 – February 2015	*35 ± 12 million m^3*	*14 ± 10 million m^3*
February 2015 – November 2018	*7 ± 6 million m^3*	*12 ± 16 million m^3*
Submarine Lobe (2008-18) (volume of sediment deposited during the time-lapse surveys)	- (no discernible erosion)	30 ± 38 million m^3 (i.e. deposited volume)
Total	66–84 million m^3	49 million m^3
	Deficit of 17–35 million m^3 of sediment over the entire system, which may include deposits outside channel that are too thin to resolve with available bathymetry survey resolution, or delta progradation upstream of the extent of the surveys.	

the multibeam bathymetry of 0.5% of the water depth (Heijnen et al., 2020). Sediment released through erosion as well as sediment delivered by the rivers were regarded as sediment sources, and were compared to the volumes of the depositional zones. In order to compare the depositional volumes derived from difference mapping with the sediment supplied by the feeding rivers, we convert the annual range in sediment supply for the Homathko River (from Syvitski and Farrow, 1983) to sediment volumes, using a porosity range of 0.3–0.6 (Beard and Weyl, 1973; Houston et al., 2011) and a sediment density of 2,585 kg/m^3 (97% sand, 3% organics; Syvitski and Farrow, 1983). Comparison between these two values allows determination of how much of the sediment supplied by the rivers accumulated within the submarine channel system. No sediment input data are available for the Southgate River, but we expect it to be small as its discharge is estimated to be only 19–36 % of that of the Homathko River.

5. Results

5.1. Bathymetric and volumetric changes between 2008 and 2018

The submarine channel-lobe system is morphologically dynamic along its full length. All sections apart from the lobe experienced some resolvable erosion or deposition over the ten years. Approximately 30% of the channel underwent at least 5 m of elevation change (Fig. 3c). Erosion locally exceeded 30 m, with deposition exceeding 10 m in some parts. Sediment budget analysis suggests a net removal of 17–35*10^6 m^3 sediment from the system (Table 1). Section 6.3 discusses the likely fate of this apparently missing sediment. The main removal of sediment originates from the channel, while the sediment input from the river approximately matches the deposition on the lobe (Table 1; Syvitski and Farrow, 1983).

5.2. Change on the prodeltas and in the channel

A complex pattern of erosion and deposition characterises the Homathko prodelta and most-upstream part of the channel, primarily resulting from the upstream-migration of crescentic bedforms (Fig. 3e), but also due to localised channel-flank collapses, terrace formation and local avulsions of the channel thalweg (Fig. 3d). Downstream of M5, an alternating pattern of erosion and deposition occurs along the length of the channel, as a result of zones of steep 10–40 m-high knickpoints that progressively migrated upstream at 100–450 m/yr. This upstream-migration of knickpoint-zones creates channel-wide erosion zones, downstream of which sediment accumulates at up to 1.1 m/yr (Fig. 3c; Heijnen et al., 2020). Where a knickpoint migrates upstream into a reach of the channel previously dominated by deposition, it can completely remove any prior evidence of deposition; with the resultant stratigraphy locally indicating an apparent balance between erosion and deposition (Fig. 4). The overall eroded volume exceeded the deposited volume in the channel by 22*10^6 m^3 (Table 1). The eroded volume was largest between November 2010 and February 2015. Volumes of seabed change appear more balanced in the other periods, but are close to the uncertainty threshold (0.5% of water depth; Table 1).

5.3. Change on the lobe

The lobe grew by 30*10^6 m^3 of sediment between March 2008 and November 2018, which locally reached 10 m thickness (Fig. 5a, b). Most of this deposition occurred between November 2010 and February 2015. Up to 6 m of deposition occurred between November 2014 and June 2014, and up to 3 m between June 2014 and February 2015. No deposition was detected on the lobe from November 2015 to 2018; at least not above the vertical accuracy of the multibeam data. Therefore, significant and resolvable sediment delivery to the lobe only occurred in 4 of the 11 yrs observed. The transition between the channel and the lobe is characterised by a ~15 m-high knickpoint (Fig. 5a, b). This knickpoint migrated 2.1 km upstream between March 2008 and November 2018. A down-dip profile along the lobe reveals a lenticular depositional morphology, the thickest parts of which tend to backstep up-slope towards the channel, but also include thinner prograding bodies. Lateral expansion of the lobe is likely limited by the confinement provided by the steep fjord side walls.

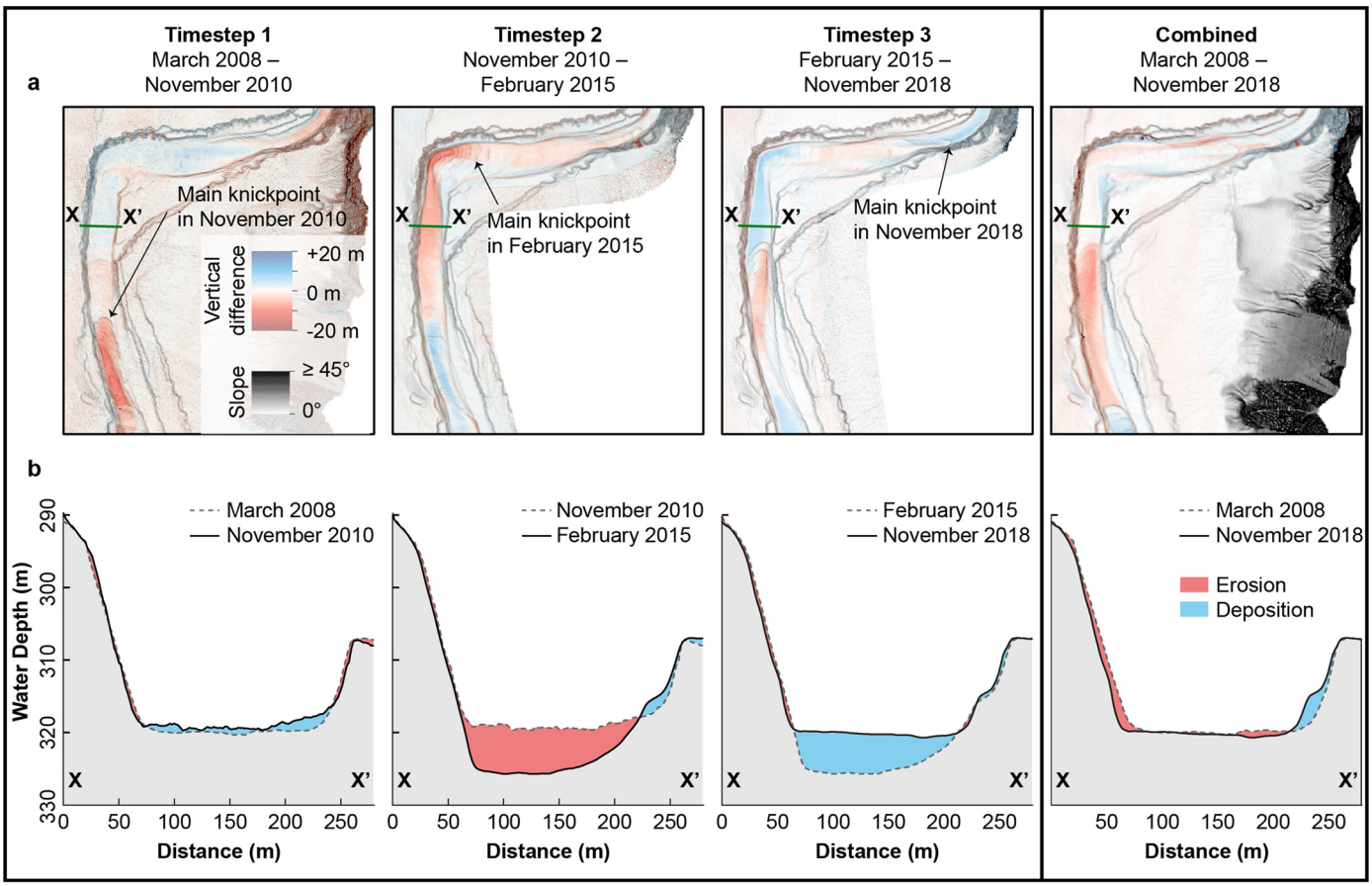

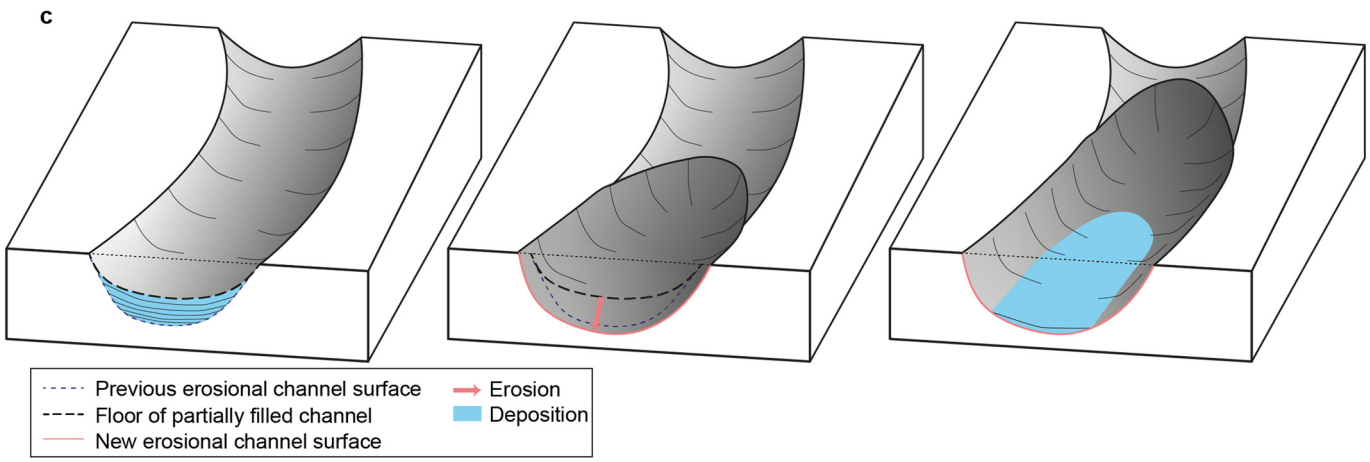

Step 1: Previously created erosional channel form is filled by sub-horizontal beds deposited by successive turbidity currents.

Step 2: An upstream migrating knickpoint erodes previously deposited sediment and creates a new channel form. The difference between the previous and new erosional channel form can vary, and determines channel evolution.

Step 3: Deposition in the channel reconvenes as the knickpoint migrates further upstream. Cycle repeats from here.

Fig. 4. Timelapse difference maps and cross sections of an area affected by knickpoint-related erosion and deposition. a) Difference maps over three time intervals compared to the difference map over the entire survey area. Location shown in Fig. 2c. Note how the erosional and depositional areas shift over time as the knickpoint migrates. b) Cross section through the channel showing changes over time compared to the change over the entire survey. Location shown in panel a. Note how the area of cross section is characterised by both phases of erosion and deposition that balance out over time. d) Schematic model showing how knickpoint related erosion and deposition can cause channel bypass over longer timescales.

5.4. Turbidity current runout distances

The ADCPs recorded 113 turbidity currents over the two summers when moorings were deployed (2016 and 2018; Fig. 6a). The number of flows recorded decreases with increasing distance along the channel (Fig. 6a, b). Most flows (92%) dissipated within the proximal part of the channel. Six flows reached M3, while only two of the 113 flows reached mooring M1 on the lobe. Most of the flows were recorded in 2018 (N=95); due to the shallowest mooring (M6) being located further downstream in 2016, and the

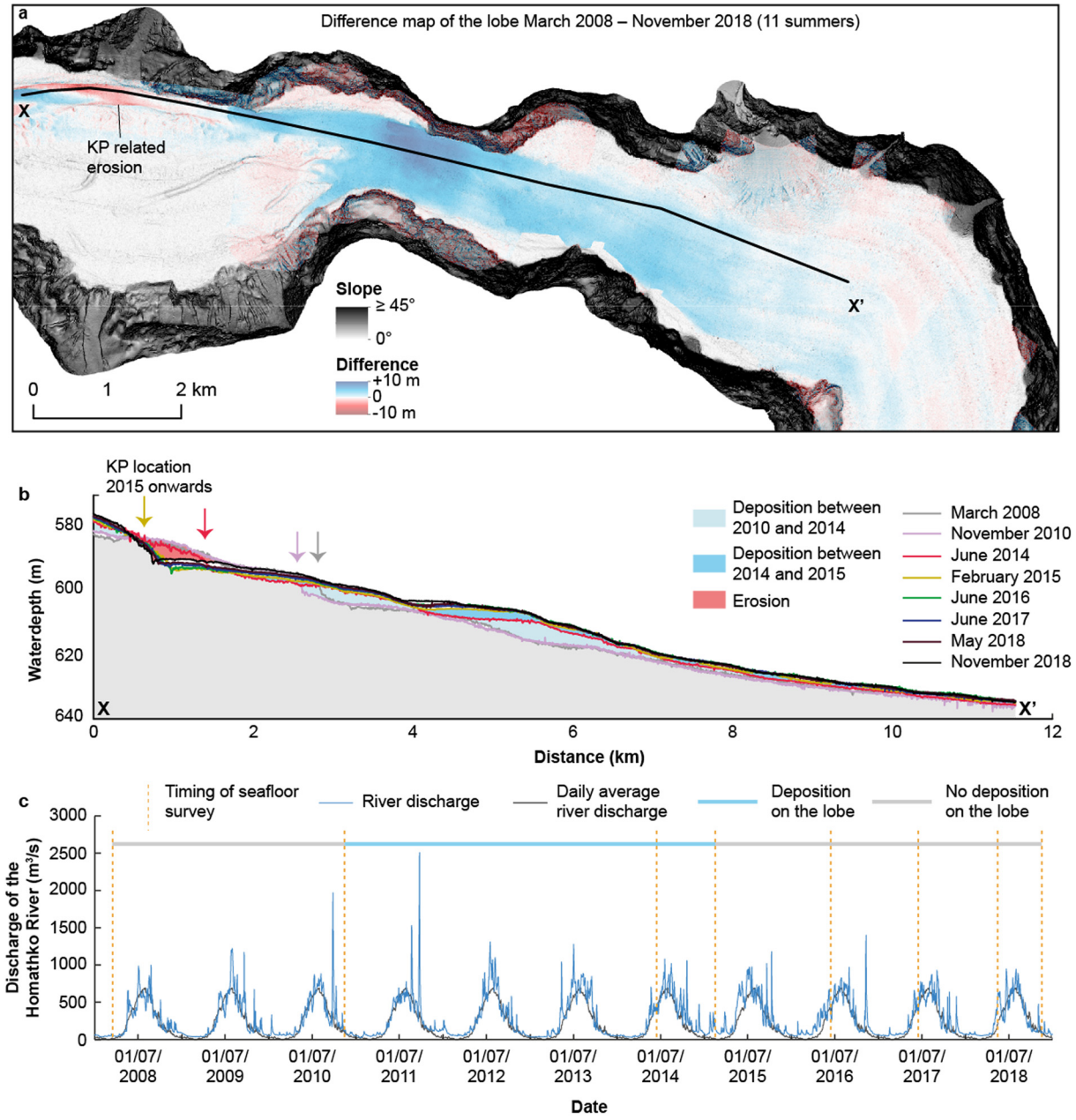

Fig. 5. Deposition on the lobe and discharge of the system's feeding river. a) Difference map showing deposition on the lobe over the entire survey. Location shown in Fig. 2c. b) Cross section showing deposition on the lobe over time. Note the deposition occurs almost exclusively between November 2010 and February 2015. c) River discharge of the Homathko River, which feeds the submarine channel-lobe system in Bute Inlet. Timings of the seafloor surveys are indicated. Two main surges occurred over the survey period, in 2010 and in 2011.

2016 mooring failing halfway through the deployment. Six flows in 2018 were recorded at M5, but not at M6. This can be attributed to M6 missing the flows starting at the Southgate River in 2018, since the M6 mooring was located upstream of the confluence of the Homathko and Southgate Delta-channels in 2018, but located downstream in 2016 (Fig. 3c; 6a). These six flows are excluded from this analysis, as it would bias the amount of flows reaching M5 compared to M6.

5.5. Variations in river discharge

Discharge of the Homathko River was seasonally-variable (Fig. 5c), with discharge in winter typically below 100 m^3/s, while summer discharge was typically above 500 m^3/s, and occasionally >800 m^3/s. The average discharge of the Homathko River over the study period was 277 m^3/s; 9% higher than previously reported by Syvitski and Farrow (1983). Larger variations between years occurred on daily-weekly timescales, with the coefficient of variation of the average daily discharge being 0.48. The two largest peaks in discharge (up to ~2,500 m^3/s) occurred in September 2010 and September 2011.

6. Discussion

We now first discuss how sediment is transported in a series of successive time steps along the channel, and when sediment is transported to the lobe in Bute Inlet. Second, we explore the potential causes for the sporadic lobe-building episodes. Third, we discuss the overall sediment budget of the system. Fourth, we use our field data to test previous models of sediment transport in

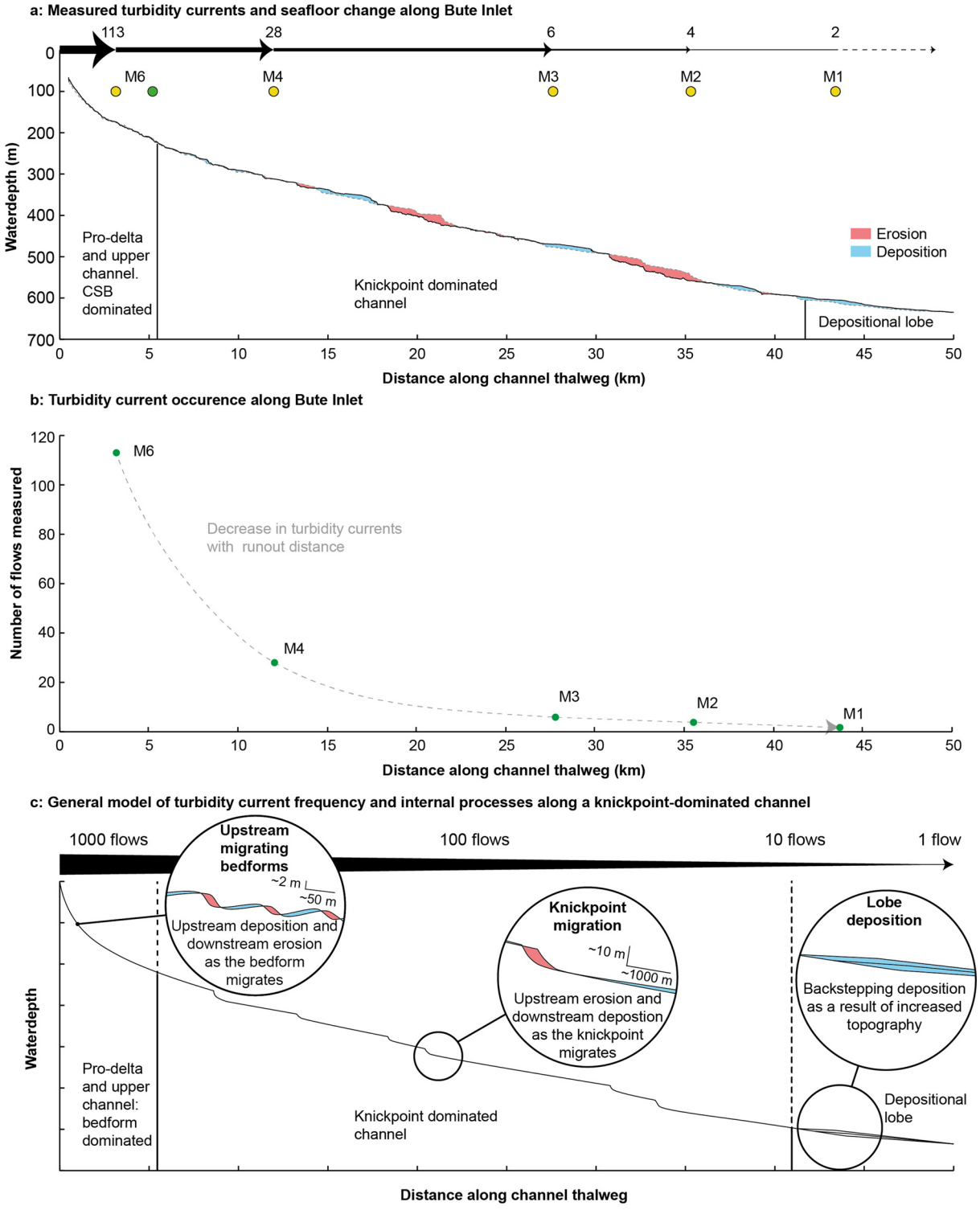

Fig. 6. Generalised model for flow magnitude-frequency-runout, and thus sediment transfer, through a submarine channel-lobe system, based on observations from Bute Inlet. a) Number of flows recorded by the ADCP at each moored station. Locations of the moorings are shown on a longitudinal profile along the channel thalweg and over the lobe. Location of M6 in 2016 in green. The longitudinal profile also shows the bathymetric difference between March 2008 and November 2018. b) Number of flows recorded at each mooring, plotted against the distance along the channel thalweg. Note the decrease of flows with distance along the channel. c) Schematic diagram showing the relative flow frequency and the dominant depositional and erosional processes along a knickpoint-dominated channel.

submarine channels and discuss whether our findings are more broadly applicable to other deep-sea systems. Fifth, we present a new model that can explain how the upstream migration of knickpoint-zones can generate bypass zones in submarine channels. Finally, we discuss the implications for the fate of land-derived material in the deep-sea, preservation of environmental signals in submarine channel deposits, and geohazard assessment for seafloor infrastructure.

6.1. Multi-stage 'shuffling' of sediment along the submarine channel-lobe system

Sediment is shuffled along the submarine channel system in several steps. The residence time in each step is controlled by the frequency and magnitude of flows, which in turn varies as a function of distance down-channel. Sediment is transported and reworked in the proximal (first ~10 km) channel system by small flows that occur frequently (10s of flows a year). Most flows dissipate over relatively short runout distances (< 12 km from source; i.e. before M5), depositing and reworking sediment in the upper reach of the system, which is characterised by migration of crescentic bedforms (Chen et al., 2021; Hughes Clarke, 2016; Vendettuoli et al., 2019), terrace formation and lateral migration of the main channel, and channel-flank failures (Fig. 3d, e).

Sediment is then transported further down-channel (~10–35 km) by less frequent flows (~10 flows per year) that typically dissipate somewhere within the channel (between M5 and M1). These flows trigger the upstream-migration of knickpoints, which are common in Bute Inlet. Sediment is deposited and stored temporarily between 'knickpoint-zones' along the channel, before being eroded via up-channel movement of the next knickpoint-zone, a process which dominates channel evolution (Fig. 4; Heijnen et al., 2020). The rate of knickpoint migration does not appear to obviously relate to the frequency of turbidity currents, and it is therefore likely that only certain types of turbidity current result in knickpoint migration (Chen et al., 2021; Supplementary Material).

The residence time of particles within the prodeltas and submarine channel is variable, and depends on where (and how often) a particle is buried. The particles that make up a flushing event might never be buried, and can be transferred straight from the river-plume to the lobe. However, most particles will be deposited in the prodelta, and will be reworked here several times by frequent turbidity currents that cause the upstream migration of crescentic bedforms. Individual bedform crests can be tracked in surveys at the start and end of a freshet season (Fig. 3e), which suggests that these bedforms migrate less than one wavelength per season. This suggests that particles can reside and be reworked within the prodelta and uppermost channel for up to a few 100s of years. Particles then reach the main part of the channel where they likely reside in the depositional zones between the knickpoint-zones. Based on migration rates, a knickpoint-zone will reach the current position of the next knickpoint-zone upstream in 17–62 yrs (supplementary material). In turn, this suggests a similar time of 17-62 yrs for sediment to reside in each depositional area between knickpoint-zones. Our data do not allow us to ascertain precisely where and how knickpoints originate. However, it is plausible that they may initiate at the channel-lobe transition, and then progressively migrate up the channel. Longer duration time-lapse surveys are required to capture the inception of a knickpoint.

Flow monitoring in 2016 and 2018 suggests ~1 turbidity current reaches the lobe each year, but these monitored flows did not leave resolvable deposits on the lobe (Fig. 5 a, b; 6a, b). Repeat surveys show that deposition on the lobe was sporadic; almost exclusively within 4 of the 11 monitored summers (November 2010 to February 2015). This lobe-building interval coincides with high erosion rates in the channel (Table 1). There may therefore be an even larger type of flow event, not captured during our flow monitoring in 2016 and 2018, that occurs in Bute Inlet on the order of once every 10 yrs, and flushes large amounts of sediment onto the lobe. Longer-term monitoring is required to record and understand such infrequent events.

6.2. What controls episodic sediment delivery to the lobe?

It is possible that such lobe-building events could be triggered by external events (e.g. floods, earthquakes or landslides). However, comparison of the timing of channel flushing and lobe aggradation between November 2010 and February 2015 with other external events does not reveal an obvious link. An unusually large flood (up to 2500 m^3/s) on the Homathko River occurred in 2011, and may explain 6 m of lobe aggradation between November 2010 and June 2014 (Fig. 5). However, the second largest flood (up to 2000 m^3/s) on the Homathko River, which occurred in 2010, did not result in any resolvable lobe deposition. Furthermore, the period between June 2014 and February 2015 accounts for the thickest annual deposition rate on the lobe, but no major flood occurred on the Homathko River during this period (Fig. 5c). It is possible that flooding on the Southgate River, which provides a secondary source of sediment, may also play a role. While the Southgate Prodelta was not surveyed between June 2014 and May 2018, no major changes in the morphology of the prodelta were observed between these surveys; hence a major flood on the Southgate River is not considered likely. Although earthquakes occur frequently along the Cascadian Margin, Juan de Fuca Ridge, and Cascade Range, no clear pattern in monitored earthquakes can directly explain the enhanced deposition on the lobe between 2010 and 2015, nor the lack of deposition in the 2008–2010 and 2015–2018 periods (Supplementary Table 1; Supplementary Fig 1). A channel-flank failure occurred between November 2010 and June 2014, which may instead explain the lobe aggradation between 2010 and 2014, but no equivalent failure occurred to explain aggradation between 2014 and 2015 (Fig. 3c,d). Therefore, no consistent trigger is identified, nor are the direct effects of a major external event necessarily required for lobe aggradation.

Alternatively, lobe-building flows might be part of the same frequency-magnitude distribution as the other flows, generated by internal (autogenic) processes, rather than by external triggers. One potential mechanism involves preconditioning of the upper channel reaches with poorly-consolidated sediment that is episodically entrained by overriding flows, causing ignition (self-acceleration), and thus enabling long runout to the lobe. In this scenario, flushing flows that build the lobe can only occur once a sufficient stock of surficial sediment has accumulated in the upper channel. Availability of suitable sediment can determine flow ignition and runout distance, particularly where easily-eroded sediment accumulates seasonally (Bailey et al., 2021; Hage et al., 2019; Heerema et al., 2020). However, it is unclear how erodible sediment that may generate flushing flows could have accumulated preferentially between 2010 and 2015, and not during other periods, given the persistent flow activity in the upper channel (Fig. 2d, e; 6a, b).

Another hypothesis is that a certain configuration of knickpoints may favour longer-runout turbidity currents. As turbidity currents flow over and erode steep knickpoints, they may also ignite and accelerate, while lower gradient relief reaches between knickpoints are depositional, and hence turbidity currents decelerate there (Chen et al., 2021; Guiastrennec-Faugas et al., 2021). A configuration in which the lower relief reaches between knickpoint-zones are shortest might thus favour flows reaching the lobe. However, we did not observe obvious knickpoint configurations that would favour sediment delivery to the lobe between November 2010 and February 2015. Increased knickpoint migration rates and channel erosion did occur between 2010 and 2015 (Heijnen et al., 2020), suggesting flows likely ignited as they traversed the system. However, it is not possible to disentangle whether this enhanced knickpoint migration rate and erosion between 2010 and 2015 is a cause or result of flushing events. Future longer-term monitoring is needed to conclude how and which flows cause lobes to aggrade. Coring of the lobe deposits can pro-

vide longer records, and may also be used to determine whether the type of aggradation episodes documented here occurred in one or multiple flow events.

6.3. First detailed source to sink sediment budgets for a submarine channel-lobe system

Overall volumes of seafloor change, combined with estimated sediment input by the Homathko River indicate a total deficit of 17–35*10^6 m^3 of sediment (Table 1). Assuming this deficit is not entirely caused by measurement uncertainties, it is conceivable this missing sediment may have accumulated on the overbank areas, and beyond the lobe. Deposits on the overbanks and up to 10 km past the lobe would need to be 18–37 cm thick on average to fully account for the missing sediment, which would be below the vertical resolution of the multibeam surveys, making this hypothesis plausible.

The overall deposition in the channel and on the lobe combined exceeds the overall erosion in the channel by around 8*10^6 m^3 between March 2008 and November 2018. This is equal to 19–32% of sediment input from the main feeding river, suggesting the remaining 68–81% is not captured and buried by the submarine channel system. Alternatively, the budget analysis shows that the lobe has grown by a volume equal to that of the estimated sediment input from the rivers. If we then assume that most of the missing volume in the sediment budget is stored as thin deposits on the overbanks and in the distal lobe, this mass balance indictes the system is approximately in equilibrium over decadal timescales.

6.4. Testing the three generalised models of sediment transport through submarine channels

We now test three fundamental models for how sediment is carried into the deep-sea, and how flow frequency-magnitude changes with distance (Fig. 2). First, we consider data from this uniquely detailed study of Bute Inlet, which spans an 11 yr period. We then discuss less detailed datasets on flow magnitude-frequency from other submarine flow systems, to consider processes that act over even longer (than decadal) timescales.

Observations of sediment transport through the submarine channel-lobe system in Bute Inlet differ in various respects from the 'ignition-autosuspension-deposition' model and the 'fill-and-flush model', while having many similarities with the 'shuffle-and-flush' model. Our results from Bute Inlet differ from the 'ignition-autosuspension-deposition' model, primarily as turbidity currents occur without catastrophic external triggers, which has also been observed in other systems (Bailey et al., 2021; Hage et al., 2019). Furthermore, the 'ignition-autosuspension-deposition' model suggests that turbidity currents typically flow through the entire length of a submarine channel system. However, our results from Bute Inlet, and other recent studies, show that turbidity currents often do not reach the lobe, with turbidity current frequency decreasing with distance along the system (Heerema et al., 2020; Stacey et al., 2019). Lastly, the 'ignition-autosuspension-deposition' model suggests turbidity currents flow in a state of autosuspension through large parts of channels, with no net erosion or deposition (Stevenson et al., 2015). Our data from Bute Inlet show that turbidity currents interact strongly with local features, such as knickpoints, creating locally-variable erosion and deposition. Turbidity currents are thus not in some state of equilibrium over long distances, nor over small timescales.

The 'fill-and-flush' model suggested a bimodal flow distribution; however, our results from Bute Inlet show a range of runout distances, which has also been shown in other systems (Heerema et al., 2020; Stacey et al., 2019). Although we observe some flushing events in Bute Inlet, these are not necessarily triggered by large external events, and may instead be internally generated, via processes that are as yet poorly understood.

Our observations from Bute Inlet show most agreement with the modified 'shuffle-and-flush' model (Fig. 2c; Paull et al., 2005). A full spectrum of flow runout lengths from proximal to distal continuously reworks and transports sediment along the length of the channel system. This preconditions the system for flows to ignite, and transport sediment to the lobe. We provide the first observations of how the upstream-migration of knickpoints can be an important process for transfer sediment along the submarine channel in a 'shuffle-and-flush' type model (Fig. 2c). We recognise, however, that other systems can have different morphologies and may thus be dominated by other processes, such as lateral migration of channel bends, localised damming by delta or channel flank collapses, and that combinations of these processes and model types may and can exist (e.g. Sylvester et al., 2011; Corella et al., 2016; Covault et al., 2019; Vendettuoli et al., 2019; Tek et al., 2021). Regardless, we suggest knickpoints can play a key, but previously overlooked, role in step-wise sediment transfer in many submarine channels given their growing recognition from seafloor surveys worldwide (e.g. Paull et al., 2011; Heijnen et al., 2020; Guiastrennec-Faugas et al., 2021).

6.5. Sediment transport over longer timescales and comparison to other submarine fan systems

It is important to note that the recurrence time of turbidity currents can be shorter in Bute Inlet compared to other active deep-sea submarine channel systems (e.g. Sequeiros et al., 2019; Bailey et al., 2021). Therefore, other factors may affect the tempo of sediment transport to the deep-sea over longer periods for such systems. For example, flushing events that build the lobe in Bute Inlet likely have a recurrence of approximately 5-10 yrs, but flushing flows can be much larger and less frequent in other systems, sometimes with recurrences of tens to thousands of years. This may potentially result from distinctly different triggers that include major external events such as earthquakes (Allin et al., 2016; Jobe et al., 2018; Mountjoy et al., 2018). However, major river-fed deep-sea systems such as the Congo Canyon have been shown to feature a comparable recurrence (Azpiroz-Zabala et al., 2017). Furthermore, as many deep-sea channels also contain evidence for a range of variable runout flows, we suggest the 'shuffle-and-flush' model could also hold for such systems, albeit potentially on longer timescales (Allin et al., 2016; Jobe et al., 2018).

On even longer timescales (>1000s yr), major system-modifying events may occur, affecting larger spatial scales than those of crescentic bedforms and knickpoints. Such larger-scale and less-frequent events include channel avulsions, landslide damming, outburst-floods, or glacially-driven sea-level cycles that may move river mouths closer to canyon heads, cut off or re-divert sediment supply, or otherwise strongly affect the transfer of sediment to the deep-sea (Jobe et al., 2015; Picot et al., 2019; Piret et al., 2022). There may be significant processes that are not captured in our 11 yr study of Bute Inlet, which could be fundamentally important controls elsewhere. To test the wider applicability of the 'shuffle-and-flush' type model will require acquisition of additional longer time series, such as have been acquired for rivers (e.g. Biedenharn et al., 2000; Paszkowski et al., 2021). While time-lapse surveys in subaqueous systems have been rare, a growing number of datasets exist, and it is hoped this study will motivate longer term monitoring of other submarine channel systems (Smith et al., 2007; Silva et al., 2019; Guiastrennec-Faugas et al., 2021).

6.6. Bypass in submarine channels

Our observations from Bute Inlet provide a new explanation for sediment bypass that may occur in many other submarine channels. Bypass is commonly used as a spatial term, referring to areas where erosion and deposition are in balance. However, bypass is also used to describe a single turbidity current, that is neither erosive nor depositional at a certain location along a submarine channel system (i.e. 'bypassing flow'; Stevenson et al., 2015). The migration rates of knickpoints in Bute Inlet ensure that total removal of previously accumulated channel fill can occur within decadal timescales, resulting locally in net zero accumulation (Fig. 3c; 4; Supplementary material). However, the timescale of surveys is too short to observe whether erosion and deposition associated with entire upstream-migrating knickpoint-zones can balance, and result in larger bypass zones over longer time scale. Estimations of erosion and deposition rates associated with knickpoint-zones 2 and 3 (Fig. 3c) show that erosion and deposition are balanced around knickpoint-zone 3, whilst the erosion exceeded the deposition around knickpoint-zone 2, although still in the same order of magnitude (Supplementary material). This suggests erosion and deposition related to upstream-migrating knickpoints can generate bypass, and bypassing flows or large flushing flows are thus not always required to generate bypass in submarine channels. This knickpoint-related mechanism differs fundamentally from how bypass is generated in the 'ignition-autosuspension-depositional' and 'fill-and-flush' models (Stevenson et al., 2015). Successive autogenic migration cycles of knickpoints may be responsible for repeated cut and fill cycles commonly observed in exhumed ancient submarine channels, without a need to invoke externally-controlled variations in sediment supply (Guiastrennec-Faugas et al., 2021; Hubbard et al., 2020).

6.7. Broader implications of progressive sediment transport

Here we briefly discuss the implications of our findings for signal preservation and stratigraphic completeness in the resulting deposits, burial of particles, and geohazard assessment. Deep-sea channel-lobe deposits may provide a record of past turbidity current activity, and hence, events that triggered them (e.g. floods, earthquakes; St.-Onge et al., 2004; Masson et al., 2011). We find that only 2% of flows reach the lobe, and that lobe deposits do not provide a complete archive of turbidity current activity in the channel, which may originate via (as yet) poorly understood internal, rather than external, mechanisms. The stratigraphic completeness of prodelta channels dominated by upstream migrating crescentic bedforms, similar to the Homathko and Southgate Prodeltas, has been shown to be low (<11% in one year; Vendettuoli et al., 2019). Based on erosion and aggradation rates in Bute Inlet, we conclude that stratigraphic completeness is even lower (1–5%; Supplementary material) over decadal to centurial timescales in the well-developed submarine channel due to upstream migration of knickpoints. This low stratigraphic completeness, which results from stepwise shuffling of sediment down the channel, has important implications for the burial of organic carbon and ultimate fate of pollutants. Modern submarine channel deposits are hotspots for organic carbon and pollutant accumulation (Azaroff et al., 2020; Baudin et al., 2010; Hage et al., 2020; Pierdomenico et al., 2020). However, we show that these deposits can be re-excavated several times before final burial. The typical pathway of a particle starts with initial deposition in the upstream part of the system by a small flow (Fig. 6c). Particles can be reworked multiple times in the proximal part of the system by frequent small flows, before re-excavation by a bigger flow that deposits this sediment within a depositional zone between knickpoint-zones. Particles are then re-excavated through headward erosion of knickpoint-zones, and deposited in one of the depositional zones downstream of the knickpoint. Particles remain here until re-excavated by flushing events, such as the lobe-building events that occurred between 2010 and 2015. Longer term burial outside of the lobe may also occur on the overbanks, terraces, prodelta, or as part of the small fraction of sediment that is not re-excavated by successive upstream-migrating knickpoints (Vendettuoli et al., 2019).

Our findings have two main implications for geohazards that threaten seafloor infrastructure. First, flow monitoring in Bute Inlet, and in other systems, shows that turbidity currents are more frequent in the proximal part of submarine channel systems than in the distal part. Seabed cables or pipelines will be much more likely to experience impacts during their 20-30 yr design life where they cross these proximal sections (Heerema et al., 2020; Stacey et al., 2019). However, flows can ignite and become more powerful as they travel down submarine channels (Heerema et al., 2020; Heezen and Ewing, 1952); hence, risk assessment for infrastructure laid across more distal reaches needs to weigh exposure to low-likelihood, but potentially high magnitude flows. Second, in addition to the direct impact of flows on a structure, knickpoint migration can excavate tens of metres of sediment, leaving seafloor infrastructure unsupported. Routing should avoid active submarine canyons and channels where possible; however, the scale of many deep-sea systems may preclude this. In such cases, areas upstream of knickpoint heads should be avoided by cable or pipeline crossings to minimise the risk of such undermining and generation of free-spans.

7. Conclusions

This study investigated the spatial and temporal patterns of sediment transport and magnitude-frequency-distance relationships of turbidity currents from source to sink in a submarine channel system, integrating repeat mapping and direct monitoring data. In contrast to previous models, we find that sediment is transported towards the lobe in multiple instances, by turbidity currents with variable runout lengths. Most flows do not reach the lobe, but rework and shuffle sediment further down the channel. Episodic large events then flush the channel and ultimately transport sediment onto the lobe. These flushing events can occur without obvious triggers, and may be internally generated. Lobe deposition appears to approximately balance sediment delivery by rivers into the system in Bute Inlet. However, if erosion within the channel is also taken into account, there appears to be a net deficit of sediment mass, which is most likely explained by uncertainties in repeat seafloor mapping. Our observations also illustrate how sediment bypass can occur in submarine channels. We show that repeated deposition and erosion generated by upstream-migrating knickpoints can balance, thus resulting in sediment bypass on decadal time-scales, without the need for sediment bypass by individual flows. The high amount of reworking, and the relatively low number of flows, reaching the lobe holds important implications for organic carbon and pollutants, which may undergo several stages of burial and re-excavation before reaching their final burial site. It is hoped that this study stimulates long-term repeat timelapse surveys in other submarine channels to understand the applicability of this new 'shuffle-and-flush' model, and better constrain the fluxes of sediment, carbon and pollutants to the deep sea. We suggest that the progressive shuffling of sediment to the lobe may be a common signature in many other submarine channels worldwide.

Data availability

Discharge data for the Homathko River are available from https://wateroffice.ec.gc.ca; station 08GD004. The timings of mea-

sured turbidity currents and their runout are included as supplementary material. Multibeam bathymetric data are held by the Geological Survey of Canada and Canadian Hydrographic Survey and are available from the corresponding author upon reasonable request.

CRediT authorship contribution statement

Maarten S. Heijnen: Data curation, Formal analysis, Investigation, Visualization, Writing – original draft. **Michael A. Clare:** Conceptualization, Funding acquisition, Investigation, Methodology, Project administration, Resources, Supervision, Writing – review & editing. **Matthieu J.B. Cartigny:** Conceptualization, Investigation, Methodology, Writing – review & editing. **Peter J. Talling:** Conceptualization, Funding acquisition, Investigation, Methodology, Project administration, Resources, Supervision, Writing – review & editing. **Sophie Hage:** Formal analysis, Investigation, Writing – review & editing. **Ed L. Pope:** Data curation, Formal analysis, Writing – review & editing. **Lewis Bailey:** Data curation, Formal analysis, Writing – review & editing. **Esther Sumner:** Conceptualization, Investigation. **D. Gwyn Lintern:** Conceptualization, Funding acquisition, Investigation, Methodology, Project administration, Resources. **Cooper Stacey:** Conceptualization, Funding acquisition, Investigation, Methodology, Project administration, Resources. **Daniel R. Parsons:** Conceptualization, Funding acquisition, Investigation, Methodology, Resources. **Stephen M. Simmons:** Formal analysis, Investigation, Methodology. **Ye Chen:** Formal analysis, Investigation, Writing – review & editing. **Stephen M. Hubbard:** Investigation, Writing – review & editing. **Joris T. Eggenhuisen:** Investigation, Writing – review & editing. **Ian Kane:** Writing – review & editing. **John E. Hughes Clarke:** Conceptualization, Data curation, Formal analysis, Investigation, Methodology, Resources.

Declaration of competing interest

The authors declare that they have no known competing financial interests or personal relationships that could have appeared to influence the work reported in this paper.

Acknowledgements

MSH was supported by European Union's Horizon 2020 research and innovation programme under the Marie Skłodowska-Curie grant agreement No. 721403. MSH and MAC acknowledge funding through Climate Linked Atlantic Sector Science - NERC National Capability programme (NE/R015953/1). MAC, MJCB, and PJT acknowledge funding from the Natural Environment Research Council (NERC), including "Environmental Risks to Infrastructure: Identifying and Filling the Gaps" (NE/P005780/1), and "New field-scale calibration of turbidity current impact modelling" (NE/P009190/1). MJBC was support by a Royal Society Research Fellowship (DHF\R1\180166). Talling was supported by a NERC and Royal Society Industry Fellowship hosted by the International Cable Protection Committee. The authors also acknowledge discussions with collaborators as part of Talling's NERC International Opportunities Fund grant (NE/M017540/1) "Coordinating and pump-priming international efforts for direct monitoring of active turbidity currents at global test sites". ELP was supported by a Leverhulme Trust Early Career Fellowship (ECF-2018-267). SH has received funding from the European Union's Horizon 2020 research and innovation programme under the Marie Sklodowska-Curie grant agreement No 899546. We further thank the Canadian Geological Survey and Canadian Hydrographic Survey for data collection and processing, in particular Peter Neelands and Brent Seymour. We also thank the captains and crew of CCGS *Vector*. We thank two reviewers and the editor for helpful and constructive comments that improved the manuscript.

Appendix A. Supplementary material

Supplementary material related to this article can be found online at https://doi.org/10.1016/j.epsl.2022.117481.

References

Allin, J.R., Hunt, J.E., Talling, P.J., Clare, M.A., Pope, E., Masson, D.G., 2016. Different frequencies and triggers of canyon filling and flushing events in Nazaré Canyon, offshore Portugal. Mar. Geol. 371, 89–105. https://doi.org/10.1016/j.margeo.2015.11.005.

Azaroff, A., Miossec, C., Lanceleur, L., Guyoneaud, R., Monperrus, M., 2020. Priority and emerging micropollutants distribution from coastal to continental slope sediments: a case study of Capbreton Submarine Canyon (North Atlantic Ocean). Sci. Total Environ. 703, 135057. https://doi.org/10.1016/j.scitotenv.2019.135057.

Azpiroz-Zabala, M., Cartigny, M.J.B., Talling, P.J., Parsons, D.R., Sumner, E.J., Clare, M.A., Simmons, S.M., Cooper, C., Pope, E.L., 2017. Newly recognized turbidity current structure can explain prolonged flushing of submarine canyons. Sci. Adv. 3, e1700200. https://doi.org/10.1126/sciadv.1700200.

Bagnold, R.A., 1962. Auto-suspension of transported sediment; turbidity currents. Proc. R. Soc. A, Math. Phys. Eng. Sci. 265, 315–319. https://doi.org/10.1098/rspa.1962.0012.

Bailey, L.P., Clare, M.A., Rosenberger, K.J., Cartigny, M.J.B., Talling, P.J., Paull, C.K., Gwiazda, R., Parsons, D.R., Simmons, S.M., Xu, J., Haigh, I.D., Maier, K.L., McGann, M., Lundsten, E., 2021. Preconditioning by sediment accumulation can produce powerful turbidity currents without major external triggers. Earth Planet. Sci. Lett. 562, 116845. https://doi.org/10.1016/J.EPSL.2021.116845.

Baudin, F., Disnar, J.-R., Martinez, P., Dennielou, B., 2010. Distribution of the organic matter in the channel-levees systems of the Congo mud-rich deep-sea fan (West Africa). Implication for deep offshore petroleum source rocks and global carbon cycle. Mar. Pet. Geol. 27, 995–1010. https://doi.org/10.1016/J.MARPETGEO.2010.02.006.

Beard, D.C., Weyl, P.K., 1973. Influence of texture on porosity and permeability of unconsolidated sand. Am. Assoc. Pet. Geol. Bull. 57, 349–369. https://doi.org/10.1306/819a4272-16c5-11d7-8645000102c1865d.

Biedenharn, D.S., Thorne, C.R., Watson, C.C., 2000. Recent morphological evolution of the lower Mississippi River. Geomorphology 34 (3–4), 227–249.

Canals, M., Puig, P., de Madron, X.D., Heussner, S., Palanques, A., Fabres, J., 2006. Flushing submarine canyons. Nature 444, 354–357. https://doi.org/10.1038/nature05271.

Carlson, P.R., Karl, H.A., 1988. Development of large submarine canyons in the Bering Sea, indicated by morphologic, seismic, and sedimentologic characteristics. Bull. Geol. Soc. Am. 100, 1594–1615. https://doi.org/10.1130/0016-7606(1988)100<1594:DOLSCI>2.3.CO;2.

Carter, L., Burnett, D., Drew, S., Marle, G., Hagadorn, L., Bartlett-McNeil, D., Irvine, N., 2009. Submarine cables and the oceans: connecting the world. J. Franklin Inst. https://doi.org/10.1016/0016-0032(79)90434-4.

Chen, Y., Parsons, D.R., Simmons, S.M., Williams, R., Cartigny, M.J.B., Hughes Clarke, J.E., Stacey, C.D., Hage, S., Talling, P.J., Azpiroz-Zabala, M., Clare, M.A., Hizzett, J.L., Heijnen, M.S., Hunt, J.E., Lintern, D.G., Sumner, E.J., Vellinga, A.J., Vendettuoli, D., 2021. Knickpoints and crescentic bedform interactions in submarine channels. Sedimentology. https://doi.org/10.1111/sed.12886.

Corella, J.P., Loizeau, J.L., Kremer, K., Hilbe, M., Gerard, J., Le Dantec, N., Stark, N., González-Quijano, M., Girardclos, S., 2016. The role of mass-transport deposits and turbidites in shaping modern lacustrine deepwater channels. Mar. Pet. Geol. 77, 515–525.

Covault, J.A., Sylvester, Z., Hudec, M.R., Ceyhan, C., Dunlap, D., 2019. Submarine channels 'swept' downstream after bend cutoff in salt basins. Depos. Rec. https://doi.org/10.1002/dep2.75. dep2.75.

Curray, J.R., Emmel, F.J., Moore, D.G., 2002. The Bengal fan: morphology, geometry, stratigraphy, history and processes. Mar. Pet. Geol. 19, 1191–1223. https://doi.org/10.1016/S0264-8172(03)00035-7.

de Leeuw, J., Eggenhuisen, J.T., Cartigny, M.J.B., 2016. Morphodynamics of submarine channel inception revealed by new experimental approach. Nat. Commun. 7, 10886. https://doi.org/10.1038/ncomms10886.

De Leo, F.C., Smith, C.R., Rowden, A.A., Bowden, D.A., Clark, M.R., 2010. Submarine canyons: hotspots of benthic biomass and productivity in the deep sea. Proc. R. Soc. B 277, 2783–2792. https://doi.org/10.1098/rspb.2010.0462.

Guiastrennec-Faugas, L., Gillet, H., Peakall, J., Dennielou, B., Gaillot, A., Jacinto, R.S., 2021. Initiation and evolution of knickpoints and their role in cut-and-fill processes in active submarine channels. Geology 49, 314–319. https://doi.org/10.1130/G48369.1.

Hage, S., Cartigny, M.J.B., Sumner, E.J., Clare, M.A., Hughes Clarke, J.E., Talling, P.J., Lintern, D.G., Simmons, S.M., Silva Jacinto, R., Vellinga, A.J., Allin, J.R., Azpiroz-Zabala, M., Gales, J.A., Hizzett, J.L., Hunt, J.E., Mozzato, A., Parsons, D.R., Pope, E.L., Stacey, C.D., Symons, W.O., Vardy, M.E., Watts, C., 2019. Direct monitoring reveals initiation of turbidity currents from extremely dilute river plumes. Geophys. Res. Lett. 46, 11310–11320. https://doi.org/10.1029/2019GL084526.

Hage, S., Galy, V.V., Cartigny, M.J.B., Acikalin, S., Clare, M.A., Gröcke, D.R., Hilton, R.G., Hunt, J.E., Lintern, D.G., McGhee, C.A., Parsons, D.R., Stacey, C.D., Sumner, E.J., Talling, P.J., 2020. Efficient preservation of young terrestrial organic carbon in sandy turbidity-current deposits. Geology. https://doi.org/10.1130/g47320.1.

Heerema, C.J., Talling, P.J., Cartigny, M.J., Paull, C.K., Bailey, L., Simmons, S.M., Parsons, D.R., Clare, M.A., Gwiazda, R., Lundsten, E., Anderson, K., Maier, K.L., Xu, J.P., Sumner, E.J., Rosenberger, K., Gales, J., McGann, M., Carter, L., Pope, E., 2020. What determines the downstream evolution of turbidity currents? Earth Planet. Sci. Lett. 532, 116023. https://doi.org/10.1016/j.epsl.2019.116023.

Heezen, B.C., Ewing, M., 1952. Turbidity currents and submarine slumps, and the 1929 Grand Banks earthquake. Am. J. Sci. https://doi.org/10.2475/ajs.250.12.849.

Heijnen, M.S., Clare, M.A., Cartigny, M.J.B., Talling, P.J., Hage, S., Lintern, D.G., Stacey, C., Parsons, D.R., Simmons, S.M., Chen, Y., Sumner, E.J., Dix, J.K., Hughes Clarke, J.E., 2020. Rapidly-migrating and internally-generated knickpoints can control submarine channel evolution. Nat. Commun. 11. https://doi.org/10.1038/s41467-020-16861-x.

Houston, J., Butcher, A., Ehren, P., Evans, K., Godfrey, L., 2011. The evaluation of brine prospects and the requirement for modifications to filing standards. Econ. Geol. https://doi.org/10.2113/econgeo.106.7.1225.

Hubbard, S.M., Jobe, Z.R., Romans, B.W., Covault, J.A., Sylvester, Z., Fildani, A., 2020. The stratigraphic evolution of a submarine channel: linking seafloor dynamics to depositional products. J. Sediment. Res. 90, 673–686. https://doi.org/10.2110/jsr.2020.36.

Hughes Clarke, J.E., 2016. First wide-angle view of channelized turbidity currents links migrating cyclic steps to flow characteristics. Nat. Commun. 7, 1–13. https://doi.org/10.1038/ncomms11896.

Inman, D.L., Nordstrom, C.E., Flick, R.E., 1976. Currents in submarine canyons: an air-sea-land interaction. Annu. Rev. Fluid Mech. 8, 275–310. https://doi.org/10.1146/annurev.fl.08.010176.001423.

Jobe, Z.R., Howes, N., Romans, B.W., Covault, J.A., 2018. Volume and recurrence of submarine-fan-building turbidity currents. Depos. Rec. 4, 160–176. https://doi.org/10.1002/dep2.42.

Jobe, Z.R., Sylvester, Z., Parker, A.O., Howes, N., Slowey, N., Pirmez, C., 2015. Rapid adjustment of submarine channel architecture to changes in sediment supply. J. Sediment. Res. https://doi.org/10.2110/jsr.2015.30.

Masson, D.G., Arzola, R.G., Wynn, R.B., Hunt, J.E., Weaver, P.P.E., 2011. Seismic triggering of landslides and turbidity currents offshore Portugal. Geochem. Geophys. Geosyst. 12. https://doi.org/10.1029/2011GC003839.

Mountjoy, J.J., Howarth, J.D., Orpin, A.R., Barnes, P.M., Bowden, D.A., Rowden, A.A., Schimel, A.C.G., Holden, C., Horgan, H.J., Nodder, S.D., Patton, J.R., Lamarche, G., Gerstenberger, M., Micallef, A., Pallentin, A., Kane, T., 2018. Earthquakes drive large-scale submarine canyon development and sediment supply to deep-ocean basins. Sci. Adv. 4, eaar3748. https://doi.org/10.1126/sciadv.aar3748.

Normark, W.R., 1970. Growth patterns of deep-sea fans. Am. Assoc. Pet. Geol. Bull. 54, 2170–2195. https://doi.org/10.1306/5D25CC79-16C1-11D7-8645000102C1865D.

Normark, W.R., Piper, D.J.W., 1991. Initiation processes and flow evolution of turbidity currents: implications for the depositional record. In: From Shoreline to Abyss: Contributions in Marine Geology in Honor of Francis Parker Shepard, pp. 207–230.

Parker, G., Pantin, H.M., Fukushima, Y., 1986. Self-accelerating turbidity currents. J. Fluid Mech. 171, 145. https://doi.org/10.1017/S0022112086001404.

Paszkowski, A., Goodbred, S., Borgomeo, E., Khan, M., Hall, J.W., 2021. Geomorphic change in the Ganges–Brahmaputra–Meghna delta. Nature Rev. Earth Environ. 2 (11), 763–780.

Paull, C.K., Caress, D.W., Ussler, W., Lundsten, E., Meiner-Johnson, M., 2011. High-resolution bathymetry of the axial channels within Monterey and Soquel submarine canyons, offshore central California. Geosphere 7, 1077–1101. https://doi.org/10.1130/GES00636.1.

Paull, C.K., Mitts, P., Ussler, W., Keaten, R., Greene, H.G., 2005. Trail of sand in upper Monterey Canyon: offshore California. Bull. Geol. Soc. Am. 117, 1134–1145. https://doi.org/10.1130/B25390.1.

Paull, C.K., Talling, P.J., Maier, K.L., Parsons, D., Xu, J., Caress, D.W., Gwiazda, R., Lundsten, E.M., Anderson, K., Barry, J.P., Chaffey, M., O'Reilly, T., Rosenberger, K.J., Gales, J.A., Kieft, B., McGann, M., Simmons, S.M., McCann, M., Sumner, E.J., Clare, M.A., Cartigny, M.J., 2018. Powerful turbidity currents driven by dense basal layers. Nat. Commun. 9. https://doi.org/10.1038/s41467-018-06254-6.

Picot, M., Marsset, T., Droz, L., Dennielou, B., Baudin, F., Hermoso, M., de Rafelis, M., Sionneau, T., Cremer, M., Laurent, D., Bez, M., 2019. Monsoon control on channel avulsions in the Late Quaternary Congo Fan. Quat. Sci. Rev. https://doi.org/10.1016/j.quascirev.2018.11.033.

Piret, L., Bertrand, S., Nguyen, N., Hawkings, J., Rodrigo, C., Wadham, J., 2022. Long-lasting impacts of a 20th century glacial lake outburst flood on a Patagonian fjord-river system (Pascua River). Geomorphology 399, 108080.

Pierdomenico, M., Casalbore, D., Chiocci, F.L., 2020. The key role of canyons in funnelling litter to the deep sea: a study of the Gioia Canyon (Southern Tyrrhenian Sea). Anthropocene 30, 100237. https://doi.org/10.1016/j.ancene.2020.100237.

Prins, M.A., Postma, G., 2000. Effects of climate, sea level, and tectonics unraveled for last deglaciation turbidite records of the Arabian Sea. Geology 28, 375. https://doi.org/10.1130/0091-7613(2000)28<375:EOCSLA>2.0.CO;2.

Prior, D.B., Bornhold, B.D., Wiseman, W.J., Lowe, D.R., 1987. Turbidity current activity in a British Columbia Fjord. Science 80 (237), 1330–1333. https://doi.org/10.1126/science.237.4820.1330.

Sequeiros, O.E., Bolla Pittaluga, M., Frascati, A., Pirmez, C., Masson, D.G., Weaver, P., Crosby, A.R., Lazzaro, G., Botter, G., Rimmer, J.G., 2019. How typhoons trigger turbidity currents in submarine canyons. Sci. Rep. 9. https://doi.org/10.1038/s41598-019-45615-z.

Shepard, F.P., 1981. Submarine canyons: multiple causes and long-time persistence. Am. Assoc. Pet. Geol. Bull. 65, 1062–1077. https://doi.org/10.1306/03B59459-16D1-11D7-8645000102C1865D.

Silva, T.A., Girardclos, S., Stutenbecker, L., Bakker, M., Costa, A., Schlunegger, F., Lane, S.N., Molnar, P., Loizeau, J.L., 2019. The sediment budget and dynamics of a delta-canyon-lobe system over the Anthropocene timescale: the Rhone River delta, Lake Geneva (Switzerland/France). Sedimentology 66 (3), 838–858.

Smith, D.P., Kvitek, R., Iampietro, P.J., Wong, K., 2007. Twenty-nine months of geomorphic change in upper Monterey Canyon (2002–2005). Mar. Geol. 236 (1–2), 79–94.

St.-Onge, G., Mulder, T., Piper, D.J.W., Hillaire-Marcel, C., Stoner, J.S., 2004. Earthquake and flood-induced turbidites in the Saguenay Fjord (Québec): a Holocene paleoseismicity record. Quat. Sci. Rev. 23, 283–294. https://doi.org/10.1016/j.quascirev.2003.03.001.

Stacey, C.D., Hill, P.R., Talling, P.J., Enkin, R.J., Hughes Clarke, J., Lintern, D.G., 2019. How turbidity current frequency and character varies down a fjord-delta system: combining direct monitoring, deposits and seismic data. Sedimentology. https://doi.org/10.1111/sed.12488.

Stevenson, C.J., Jackson, C.A.-L., Hodgson, D.M., Hubbard, S.M., Eggenhuisen, J.T., 2015. Deep-water sediment bypass. J. Sediment. Res. 85, 1058–1081. https://doi.org/10.2110/jsr.2015.63.

Sylvester, Z., Pirmez, C., Cantelli, A., 2011. A model of submarine channel-levee evolution based on channel trajectories: implications for stratigraphic architecture. Mar. Pet. Geol. 28, 716–727. https://doi.org/10.1016/j.marpetgeo.2010.05.012.

Syvitski, J.P.M., Farrow, G.E., 1983. Structures and processes in bayhead deltas: knight and bute inlet, British Columbia. Sediment. Geol. 36, 217–244. https://doi.org/10.1016/0037-0738(83)90010-6.

Tek, D.E., McArthur, A.D., Poyatos-Moré, M., Colombera, L., Patacci, M., Craven, B., McCaffrey, W.D., 2021. Relating seafloor geomorphology to subsurface architecture: how mass-transport deposits and knickpoint-zones build the stratigraphy of the deep-water Hikurangi Channel. Sedimentology 68 (7), 3141–3190.

Vendettuoli, D., Clare, M.A., Clarke, J.E.H., Vellinga, A., Hizzett, J., Hage, S., Cartigny, M.J.B., Talling, P.J., Waltham, D., Hubbard, S.M., Stacey, C., Lintern, D.G., 2019. Daily bathymetric surveys document how stratigraphy is built and its extreme incompleteness in submarine channels. Earth Planet. Sci. Lett. 515, 231–247. https://doi.org/10.1016/J.EPSL.2019.03.033.

Wells, M., Cossu, R., 2013. The possible role of Coriolis forces in structuring large-scale sinuous patterns of submarine channel-levee systems. Philos. Trans. - Royal Soc., Math. Phys. Eng. Sci. https://doi.org/10.1098/rsta.2012.0366.

Zeng, J., Lowe, D.R., Prior, D.B., Wiseman, W.J., Bornhold, B.D., 1991. Flow properties of turbidity currents in Bute Inlet, British Columbia. Sedimentology 38, 975–996. https://doi.org/10.1111/j.1365-3091.1991.tb00367.x.